An Examination of the CRASH3 Effective Mass Concept

Nathan A. Rose, Stephen J. Fenton and Richard M. Ziernicki
Knott Laboratory, Inc.

SAE®

Global Mobility Database®

All SAE papers, standards, and selected books are abstracted and indexed in the Global Mobility Database.

For multiple print copies contact:

SAE Customer Service
Tel: 877-606-7323 (inside USA and Canada)
Tel: 724-776-4970 (outside USA)
Fax: 724-776-1615
Email: CustomerService@sae.org

Positions and opinions advanced in this paper are those of the author(s) and not necessarily those of SAE. The author is solely responsible for the content of the paper. A process is available by which discussions will be printed with the paper if it is published in SAE Transactions.

Persons wishing to submit papers to be considered for presentation or publication by SAE should send the manuscript or a 300 word abstract of a proposed manuscript to: Secretary, Engineering Meetings Board, SAE.

Printed in USA

An Examination of the CRASH3 Effective Mass Concept

Nathan A. Rose, Stephen J. Fenton and Richard M. Ziernicki
Knott Laboratory, Inc.

ABSTRACT

This paper examines the validity of the effective mass concept used in the CRASH 3 damage analysis equations. In this study, the effective mass concept is described, the simplifying assumptions that it entails are detailed, and the accuracy of the concept is tested by comparing ΔVs calculated from the CRASH 3 equations to results of numerical simulations with a non-central impact model. This non-central impact model allowed the effective mass concept to be tested in isolation from other assumptions of the CRASH 3 program. The results of this research have shown that the effective mass concept accurately models the effects of collision force offset when certain conditions are met. These conditions are discussed, along with their implications for damage interpretation.

This paper also presents an analytic expression that relates damage energy to closing speed (initial relative velocity) for the general case of non-central collisions. Equations relating damage energy to closing speed for the case of central collisions have been discussed extensively in the literature. However, a comparable equation for the general case of vehicle-to-vehicle non-central impacts has not been reported. The effective mass concept is used to generalize the relationship between closing speed and damage energy.

INTRODUCTION

Using the mass-spring system shown in Figure 1, McHenry derived simple, closed-form equations that relate the energy expended in crushing a vehicle to the change in velocity experienced by the vehicle during the impact (ΔV) [5,6,7,8,9]. These equations, given by Equations (1) and (2) below, form the basis of the CRASH 3 damage analysis algorithm and are valid for the case of central collisions, where the collision forces are directed through the centers of gravity of the vehicles.

In Figure 1 and in Equations (1) and (2), M_1 and M_2 are the vehicle masses, K_1 and K_2 are the structural stiffnesses of the engaged vehicle structures, and E_1 and E_2 are the energies associated with crushing the vehicle structures.
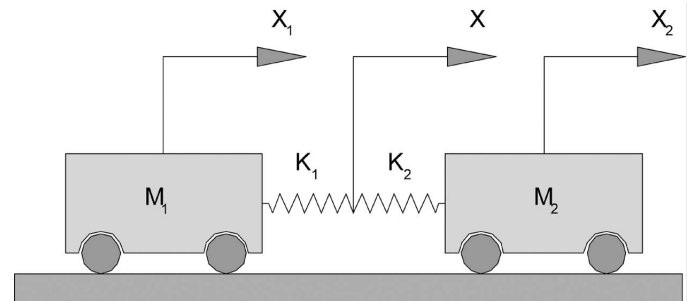

Figure 1
The CRASH 3 Impact Model

$$\Delta V_1 = \sqrt{\frac{2(E_1 + E_2)}{M_1\left(1 + \frac{M_1}{M_2}\right)}} \tag{1}$$

$$\Delta V_2 = \sqrt{\frac{2(E_1 + E_2)}{M_2\left(1 + \frac{M_2}{M_1}\right)}} \tag{2}$$

McHenry extended Equations (1) and (2) to the general case of non-central collisions using the concept of an effective vehicle mass. The effective mass concept was based on the idea that when the collision force does not pass through the center of gravity of a vehicle, the full weight of the vehicle does not participate in the collision. Application of the effective mass concept resulted in only slight modifications to the simple analytic equations derived for the central case.

McHenry began the development of the effective mass concept by considering the collision model shown in Figure 2. In this figure, I_1 and I_2 are the yaw moments of inertia of the vehicles, ψ_1 and ψ_2 are the angular orientations of the vehicles, h_1 and h_2 are the distances that the collision forces are offset from the centers of gravity of the vehicles – measured perpendicular to the line of action of the collision forces – and $\Delta V_1'$ and $\Delta V_2'$ are the changes in velocity experienced by each vehicle

at point P, the point of application of the resultant collision forces. The x_1-y_1 and x_2-y_2 frames are body-fixed reference frames. It is assumed that during the depicted collision, a common velocity is reached at the common point P, but not necessarily by the vehicle centers of gravity.
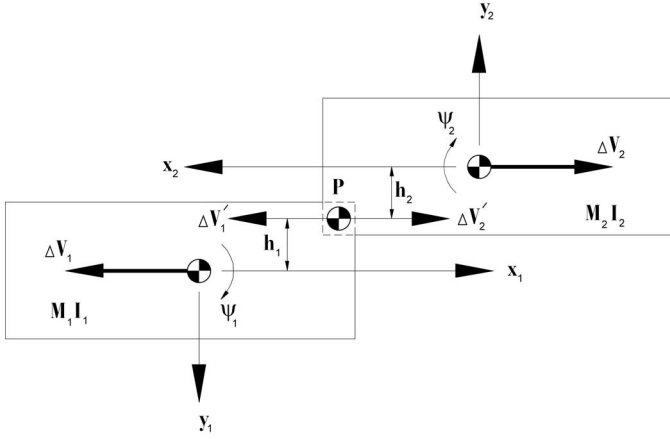

Figure 2
McHenry's Eccentric Collision Configuration

With this impact model, McHenry arrived at the following generalized equations:

$$\Delta V_1 = \sqrt{\frac{2\gamma_1 (E_1 + E_2)}{M_1 \left(1 + \frac{\gamma_1 M_1}{\gamma_2 M_2}\right)}} \tag{3}$$

$$\Delta V_2 = \sqrt{\frac{2\gamma_2 (E_1 + E_2)}{M_2 \left(1 + \frac{\gamma_2 M_2}{\gamma_1 M_1}\right)}} \tag{4}$$

In Equations (3) and (4), the multipliers, γ_1 and γ_2, are the effective mass multipliers and are given as follows:

$$\gamma_i = \frac{k_i^2}{k_i^2 + h_i^2} \tag{5}$$

In Equation (5), k_i is the radius of gyration of Vehicle 1 or 2. The validity of Equations (3) and (4), and the effective mass concept that forms their base, was the fundamental question of this study.

The effective mass concept represents an approximate method for incorporating collision forces that are offset from the vehicle center of gravity, since McHenry's derivation of Equations (3) and (4) relied on writing the acceleration of point P on Vehicle 1 as follows:

$$\ddot{X}_P = \ddot{X}_1 + h_1 \ddot{\psi}_1 \tag{6}$$

In Equation (6), $\ddot{X}_P$ is the acceleration at the point P, $\ddot{X}_1$ is the acceleration at the center of gravity of Vehicle 1, and $\ddot{\psi}_1$ is the angular acceleration of Vehicle 1.

Strictly speaking, Equation (6) is incomplete. A complete expression for the acceleration of a point on a rigid body relative to the center of gravity of that body takes the following form [1,2]:

$$\vec{a}_P = \vec{a}_G + \ddot{\psi}_1 \times \vec{r}_{P/G} + \dot{\psi}_1 \times \left(\dot{\psi}_1 \times \vec{r}_{P/G}\right) \tag{7}$$

In Equation (7), $\vec{a}_P$ is the acceleration of the point P, $\vec{a}_G$ is the acceleration of the center of gravity, $\vec{r}_{P/G}$ is a position vector that locates the point P in a reference frame attached to the body at the center of gravity, $\dot{\psi}_1$ is the angular velocity of the body about the center of gravity, and again, $\ddot{\psi}_1$ is the angular acceleration of the body about the center of gravity. The first term on the right side of Equation (7) accounts for the translational acceleration of the center of gravity relative to the inertial (fixed) frame. The second term accounts for the angular acceleration of the reference frame attached to the body. And finally, the third term accounts for the centripetal acceleration of point P. A comparison of Equations (6) and (7) reveals that Equation (6) contains no term to account for the centripetal acceleration of the point P.

Equation (7) results from taking the derivative with respect to time of the velocity expression for a point on a rigid body relative to the body center of gravity, Equation (8) below.

$$\vec{v}_P = \vec{v}_G + \dot{\psi}_1 \times \vec{r}_{P/G} \tag{8}$$

The centripetal acceleration term in Equation (7) arises during application of the chain rule during differentiation of the second term in Equation (8) and, ultimately, arises as a result of differentiating the position vector with respect to time. This is shown below in Equations (9) through (12), which show the differentiation with respect to time of Equation (8) in a series of steps. Equation (12) is equivalent to Equation (7).

$$\frac{d\vec{v}_P}{dt} = \frac{d\vec{v}_G}{dt} + \frac{d}{dt}\left(\dot{\psi}_1 \times \vec{r}_{P/G}\right) \tag{9}$$

$$\vec{a}_P = \vec{a}_G + \frac{d\dot{\psi}_1}{dt} \times \vec{r}_{P/G} + \dot{\psi}_1 \times \frac{d\vec{r}_{P/G}}{dt} \tag{10}$$

$$\vec{a}_P = \vec{a}_G + \ddot{\psi}_1 \times \vec{r}_{P/G} + \dot{\psi}_1 \times \vec{v}_{P/G} \tag{11}$$

$$\vec{a}_P = \vec{a}_G + \ddot{\psi}_1 \times \vec{r}_{P/G} + \dot{\psi}_1 \times \left(\dot{\psi}_1 \times \vec{r}_{P/G}\right) \tag{12}$$

In McHenry's derivation, h_1 and h_2 are equivalent to $\vec{r}_{P/G}$, since h_1 and h_2 are taken perpendicular to the collision force. McHenry treated h_1 and h_2 as constants. Treating the collision force moment arms as constants is an approximation, since for the system shown in Figure 2, and for actual impacts, the moment arms of the collision force will vary through time, due to variation in the direction of the instantaneous collision force and movement of the point of application of the instantaneous, resultant collision force. The significance of this for McHenry's derivation is that since he assumed the collision force moment arm does not vary with time, the centripetal acceleration term does not arise when Equation (31) is differentiated with respect to time, since the time derivative of $\vec{r}_{P/G}$ is equal to zero.

So, the fundamental assumption of the derivation of the effective mass concept is that a representative, effective, or resultant collision force moment arm can replace the time-varying collision force moment arm that is present during the actual impact. This is the assumption tested by the research reported in this paper. Various definitions of this resultant moment arm are plausible and the derivation does not specify which definition should be used. These various definitions will be explored later and the results obtained using each one will be compared.

It should be noted that McHenry's derivation of the effective mass concept is quasi-one-dimensional, meaning that, while rotational effects have been incorporated into the derivation, the change in velocity is still assumed to occur along the X-direction. This is clear from the fact the derivation involves only scalar quantities and is written in terms of X and its derivatives – Y and its derivatives do not appear. For an actual offset impact, the change in velocity will occur in more than one coordinate direction. In practice, this simply means that the one-dimensional ΔV obtained from the CRASH 3 equations will occur along the direction of the principle collision force, which for CRASH 3 analysis, the user must specify. The direction of the principle force becomes the one dimension along which McHenry's derivation is valid. This will be important later during derivation of a generalized damage energy/ closing speed formula.

VALIDATION OF THE EFFECTIVE MASS CONCEPT

To explore the physical accuracy of the effective mass concept in the CRASH 3 damage equations, the present research examined an offset barrier impact model that incorporated a collision force offset from the vehicle center of gravity. This impact model (Figure 3) consisted of a mass and a spring with the point of connection between the mass and the spring offset from the center of gravity of the mass. Also, the point of connection between the mass and the spring is enclosed in a frictionless track. The motivation for the addition of the frictionless track is the empirical observation that in an actual offset barrier collision, the vehicle center of

rotation would roughly coincide with the point where the resultant collision force is transferred, the point 1P in the barrier impact model. The track in the model forces the center of rotation to reside at the point 1P.
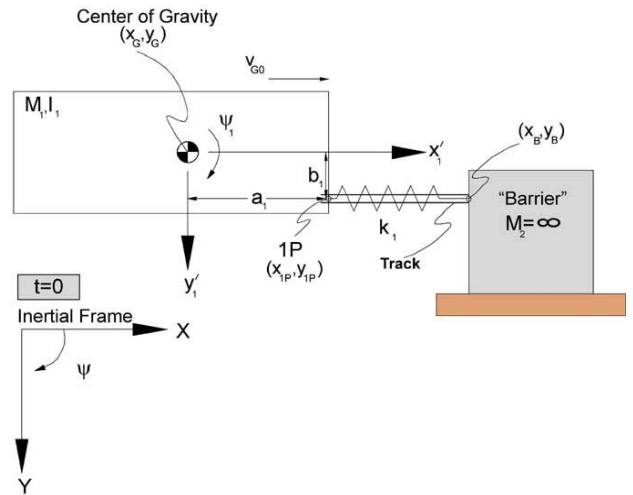

Figure 3
Offset Barrier Impact Model

Adding this track affects the system physically in two ways. First, the spring force is confined to the X-direction. Second, a Y-direction reaction force arises as a result of the interaction between the body and the track. This reaction force will cause the resultant external force (collision force) to have a component in the negative Y-direction.

The impact model of Figure 3 consists of a rectangular body of mass M_1, with yaw moment of inertia I_1, a linear spring, with stiffness coefficient k_1, and a rigid barrier of infinite mass. The center of gravity of the body is located in the inertial reference frame with the coordinates x_G and y_G and the orientation of the body is described by the angle ψ_1 measured clockwise off of the inertial x-axis. The reference frame $x_1' - y_1'$ is attached to the body and the point 1P is fixed in this reference frame at the coordinates a_1 and b_1. The spring is connected to the point 1P on the body (x_{1P} and y_{1P} in the inertial reference frame) and point B (x_B and y_B in the inertial reference frame) on the barrier.

The following assumptions are invoked for the system shown in Figure 3:

1. The point 1P is confined to move in the x-direction by the frictionless track.

2. The only forces acting on the mass are the spring force, generated by relative movement between point 1P on the body and point B on the barrier, and the constraint (reaction) force holding the point 1P in the track. Together, these constitute the "collision" force.

3. The initial translational velocity and the initial orientation of the body are in the positive x-direction.

4. The body has no initial rotational velocity.

5. At time t = 0, the spring applies no force to the body.

The barrier impact model shown in Figure 3 is a two degree-of-freedom system. A Newton-Euler formulation of the equations of motion for this system consists of the three Newton-Euler equations – one for each coordinate direction and one for rotation – augmented by a single algebraic constraint equation. The approach taken in this research for solving the equations of motion was to write the Newton-Euler equations, along with the constraint equation, and then to eliminate the unknown constraint force and redundant coordinate from the equations of motion by differentiating the constraint equation twice with respect to time and substituting it into the equations of motion. This has the effect of reducing the equations of motion to two second-order differential equations, and therefore, of simplifying the numerical solution. After the solution of these two equations, the redundant coordinate and reaction force were obtained by back-substitution.

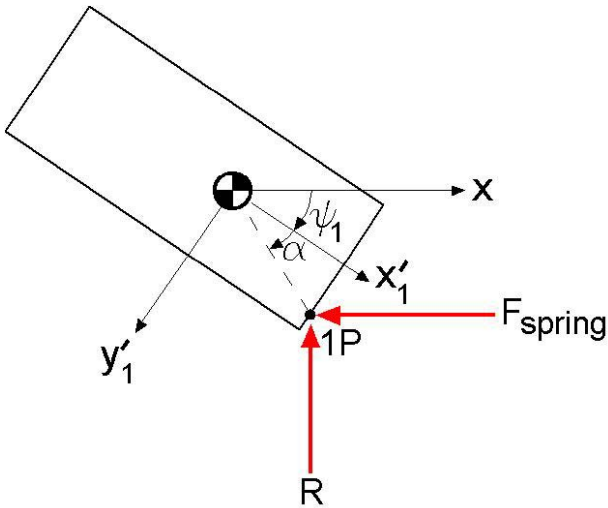A free body diagram for the mass in the offset barrier impact model follows in Figure 4.

Figure 4
Free-Body Diagram

In Figure 4, F_{SPRING} is the spring force and R is the reaction force that maintains the point 1P in the track. The magnitude of the spring force is equal to the spring stiffness k_1 multiplied by the compression of the spring beyond its equilibrium position and is given by Equation (13).

$$F_{SPRING} = k_1\left(x_{1P0} - x_{1P}\right) \tag{13}$$

In Equation (13), x_{1P0} is the initial x-direction position of the point 1P and x_{1P} is the x-direction position of the point 1P at any time, t. In terms of the coordinates of the center of gravity,

$$x_{1P0} = x_{G0} + a_1 \tag{14}$$

$$x_{1P} = x_G + a_1 \cos\psi_1 - b_1 \sin\psi_1 \tag{15}$$

In Equation (14), x_{G0} is the initial x-direction position of the mass center of gravity. The moments, M_G, about the center of gravity are given by Equation (16).

$$M_G = -F_{SPRING}\left(b_1 \cos\psi_1 + a_1 \sin\psi_1\right) + R\left(a_1 \cos\psi_1 - b_1 \sin\psi_1\right) \tag{16}$$

Now, the Newton-Euler Equations of motion for the offset barrier impact model can be written as follows:

$$m\ddot{x}_G = F_{SPRING} \tag{17}$$

$$m\ddot{y}_G = R \tag{18}$$

$$I_G\ddot{\psi}_1 = M_G \tag{19}$$

In Equations (17) through (19), $\ddot{x}_G$ is the x-direction acceleration of the mass center of gravity, $\ddot{y}_G$ is the y-direction acceleration of the mass center of gravity, and $\ddot{\psi}_1$ is the angular acceleration of the mass about the center of gravity.

To confine the point 1P to move within the track, the Newton-Euler equations of motion must be supplemented with a single constraint equation. Letting the origin of the inertial reference frame coincide with the Point B, this constraint equation can be written as follows, in terms of the center of gravity coordinates:

$$y_G + b_1 \cos\psi_1 + a_1 \sin\psi_1 = 0 \tag{20}$$

Differentiating Equation (20) twice with respect to time yields Equation (21).

$$\ddot{y}_G = b_1\ddot{\psi}_1 \sin\psi_1 + b_1\dot{\psi}_1^2 \cos\psi_1 - a_1\ddot{\psi}_1 \cos\psi_1 + a_1\dot{\psi}_1^2 \sin\psi_1 \tag{21}$$

In Equation (21), $\dot{\psi}_1$ is the angular velocity of the mass about the center of gravity. Equation (21) can be substituted into Equation (18) and the resulting equation substituted into Equation (19) to yield two second-order differential Equations for x_G and ψ_1, which can be solved using traditional numerical methods for

differential equations. The y-coordinate of the center of gravity and the reaction force from interaction with the track can then be backed out after the x-direction and the rotational coordinates have been calculated at each time step.

NUMERICAL SIMULATIONS

Test Program

Simulations were run with the barrier impact model of Figure 3 for the following five vehicle configurations:

Vehicle #1 (Miniature)
Vehicle Weight:	2469 lbs
Yaw Moment of Inertia:	1297.15 lb-ft-sec^2
Vehicle Length:	13.32 ft
Vehicle Width:	5.07 ft
Front to CG:	6.33 ft
Stiffness per Unit Width:	72.11 lb/in^2
Damage Width:	36 inches
a_1:	3.31 feet

Vehicle #2 (Sub-Compact)
Vehicle Weight:	2753 lbs
Yaw Moment of Inertia:	1736.95 lb-ft-sec^2
Vehicle Length:	14.58 ft
Vehicle Width:	5.60 ft
Front to CG:	6.94 ft
Stiffness per Unit Width:	66.38 lb/in^2
Damage Width:	36 inches
a_1:	3.62 feet

Vehicle #3 (Compact)
Vehicle Weight:	3247 lbs
Yaw Moment of Inertia:	2553.95 lb-ft-sec^2
Vehicle Length:	16.35 ft
Vehicle Width:	6.05 ft
Front to CG:	7.48 ft
Stiffness per Unit Width:	69.97 lb/in^2
Damage Width:	36 inches
a_1:	3.97 feet

Vehicle #4 (Intermediate)
Vehicle Weight:	3947 lbs
Yaw Moment of Inertia:	3632.84 lb-ft-sec^2
Vehicle Length:	17.73 ft
Vehicle Width:	6.42 ft
Front to CG:	8.23 ft
Stiffness per Unit Width:	66.7 lb/in^2
Damage Width:	36 inches
a_1:	4.26 feet

Vehicle #5 (Full-Size)
Vehicle Weight:	4565 lbs
Yaw Moment of Inertia:	4628.02 lb-ft-sec^2
Vehicle Length:	18.64 ft
Vehicle Width:	6.65 ft
Front to CG:	8.42 ft
Stiffness per Unit Width:	113 lb/in^2
Damage Width:	36 inches
a_1:	5.11 feet

The parameters for these vehicles roughly correspond to parameters for the classes from the CRASH 3 default parameters. These were used because they provide readily available and realistic representative dimensions for the simulations. The stiffness parameters are from the updated values in Reference 10. The yaw moments of inertia are calculated using the prism method.

A total of 24 simulations runs were made, distributed between the five vehicle setups. Twenty-two of the 24 runs were made with initial vehicle velocities of 60ft/s. The remaining two were run with initial velocities of 10ft/s. Numerical analysis was carried out using a fourth-order Runge-Kutta technique with time steps varying between 50 and 500 microseconds.

Simulation Results

The maximum deformation energy for each simulation run is a part of the calculation of ΔV using the CRASH 3 algorithm and so the maximum deformation energy for each simulation is summarized in Table 1 below.

Test Number	Initial Velocity (ft/s)	b_1 (ft)	Maximum Deformation Energy (ft-lb)[1]
1	10.0	0.0	3833.85
2	10.0	2.5	3403.33
3	60.0	0.0	138018.6
4	60.0	1.0	133117.7
5	60.0	2.0	118376.1
6	60.0	2.5	109972.6

Table 1a – Maximum Deformation Energies (Mini)

Test Number	Initial Velocity (ft/s)	b_1 (ft)	Maximum Deformation Energy (ft-lb)
7	60.0	0.0	153894.4
8	60.0	1.0	149.241.9
9	60.0	2.0	134556.7
10	60.0	2.5	127605.1

Table 1b – Maximum Deformation Energies (Subcompact)

Test Number	Initial Velocity (ft/s)	b_1 (ft)	Maximum Deformation Energy (ft-lb)
11	60.0	0.0	181509.3
12	60.0	1.0	176921.2
13	60.0	2.0	210284.2
14	60.0	3.0	144987.9

Table 1c – Maximum Deformation Energies (Compact)

---

[1] Maximum deformation energies in Tables 1a through 1e are approximate, but are within 1-2% of their actual values. The authors neglected to output these values in the simulation output file and to avoid having to rerun the simulations these values were calculated from other simulation output. Calculated values reported later in this paper did not rely on these approximate values, but rather on the actual simulation values.

Test Number	Initial Velocity (ft/s)	b_1 (ft)	Maximum Deformation Energy (ft-lb)
15	60.0	0.0	220639.8
16	60.0	1.0	214830.3
17	60.0	2.0	201512.4
18	60.0	3.0	180951.8
19	60.0	4.0	159974.8
20	60.0	5.0	139830.4

Table 1d – Maximum Deformation Energies (Intermediate)

Test Number	Initial Velocity (ft/s)	b_1 (ft)	Maximum Deformation Energy (ft-lb)
21	60.0	0.0	255186.3
22	60.0	1.0	250431.3
23	60.0	2.0	237351.0
24	60.0	3.0	219090.4

Table 1e – Maximum Deformation Energies (Full Size)

In order to address the accuracy of the CRASH 3 effective mass concept, two additional values were extracted from the simulation runs. First, the resultant change in velocity experienced by the body center of gravity from time zero to the time of maximum deformation was obtained. This is the value that was compared to the CRASH 3 calculated velocity changes. Second, appropriate values for the resultant collision force moment arm were calculated, since this value is needed to calculate the effective mass factors, γ, which are also used in the calculation of the velocity change with the CRASH 3 algorithm equations.

The first of these, the resultant ΔV experienced by the vehicle in each simulation run, is easily obtained from the simulation data. The results are summarized in Tables 2a through 2e below.

Test Number	Initial Velocity (ft/s)	b_1 (ft)	$\Delta V_{resultant}$ (ft/s)
1	10.0	0.0	9.97[2]
2	10.0	2.5	9.20
3	60.0	0.0	59.84
4	60.0	1.0	57.66
5	60.0	2.0	52.06
6	60.0	2.5	48.69

Table 2a – Actual Velocity Changes (Mini)

Test Number	Initial Velocity (ft/s)	b_1 (ft)	$\Delta V_{resultant}$ (ft/s)
7	60.0	0.0	59.37
8	60.0	1.0	58.05
9	60.0	2.0	53.27
10	60.0	2.5	50.18

Table 2b – Actual Velocity Changes (Subcompact)

[2] There is some numerical error in the calculated actual ΔVs. For the central impact case, b_1=0, the actual ΔV should be equal to the impact speed. Thus, part of the error in the ΔV calculations reported later is due to error in the calculation of the actual ΔV. This will be discussed later in this paper.

Test Number	Initial Velocity (ft/s)	b_1 (ft)	$\Delta V_{resultant}$ (ft/s)
11	60.0	0.0	59.66
12	60.0	1.0	58.40
13	60.0	2.0	54.36
14	60.0	3.0	49.00

Table 2c – Actual Velocity Changes (Compact)

Test Number	Initial Velocity (ft/s)	b_1 (ft)	$\Delta V_{resultant}$ (ft/s)
15	60.0	0.0	59.58
16	60.0	1.0	58.56
17	60.0	2.0	55.06
18	60.0	3.0	50.19
19	60.0	4.0	44.87
20	60.0	5.0	39.80

Table 2d – Actual Velocity Changes (Intermediate)

Test Number	Initial Velocity (ft/s)	b_1 (ft)	$\Delta V_{resultant}$ (ft/s)
21	60.0	0.0	59.28
22	60.0	1.0	58.85
23	60.0	2.0	56.16
24	60.0	3.0	52.24

Table 2e – Actual Velocity Changes (Full Size)

The second, obtaining a representative value for the collision force moment arm is not as straight forward, since it is not immediately clear what value of the moment arm is the most representative. A number of possibilities exist for defining this "average" moment arm, including the following:

1. The first possibility is to let the average moment arm, h_{avg}, equal the initial offset of the collision force (b_1). This would be expected to be the least accurate, since the initial offset is the least representative of the moment arm throughout the collision. This moment arm occurs at the beginning of the impact, when the collision force is low.

2. The second possibility is to let h_{avg} equal the arithmetic mean value of the instantaneous moment arms (the moment arm at each time step) between time zero and maximum spring compression. This average moment arm is given by

$$h_{avg} = \frac{\sum_{i=1}^{N} h_i}{N}, \qquad (22)$$

where N is the number of time steps between time zero and the maximum spring compression. We would expect this h_{avg} to be more representative than the first definition, but still not ideal since it gives equal weight to the h value at every time step.

3. Thus, the third possibility is to let h_{avg} equal a weighted average of the instantaneous moment arms between time zero and maximum spring compression. The weighting could utilize either the instantaneous resultant collision forces or the instantaneous resultant accelerations. This average moment arm is given by

$$h_{avg} = \frac{\sum_{i=1}^{N} a_i h_i}{\sum_{i=1}^{N} a_i}, \qquad (23)$$

where N is again the number of time steps between time zero and the maximum spring compression and a_i is the acceleration at each time step.

4. The fourth possibility is to let h_{avg} equal the collision force moment arm at the time the maximum force (maximum deformation) is achieved.

Ultimately, the correct choice between these four options will be the moment arm concept that reduces the error in the ΔV predicted by the CRASH 3 equations. For the barrier impact simulations, the moment arm at any instant in time is defined as the perpendicular distance between the collision force line of action and the vehicle center of gravity. The instantaneous moment arm is given by Equation (24).

$$h_i = \sqrt{a_1^2 + b_1^2}\ \sin\left(\psi_1 + \alpha_1 - \beta_2\right) \qquad (24)$$

Numerical calculations were carried out with all four of the definitions for the "average" collision force moment arm. The resulting average moment arms, along with the effective mass multipliers that these moment arms produce, are summarized below in Tables 3a through 3e.

Test Number	Definition 1 $h_{avg} = b_1$ (ft)	γ	Definition 2 $h_{avg} = h_{mean}$ (ft)	γ	Definition 3 $h_{avg} = h_{weighted}$ (ft)	γ	Definition 4 $h_{avg} = h(F_{max})$ (ft)	γ
1	0.00	1.00	0.00	1.00	0.00	1.00	0.00	1.00
2	2.50	0.73	0.81	0.96	0.81	0.96	0.83	0.96
3	0.00	1.00	0.00	1.00	0.00	1.00	0.00	1.00
4	1.00	0.94	0.64	0.98	0.65	0.98	0.74	0.97
5	2.00	0.81	1.26	0.91	1.29	0.91	1.50	0.88
6	2.50	0.73	1.56	0.87	1.60	0.87	1.88	0.83

Table 3a – Moment Arms and Effective Mass Multipliers (Mini)

Test Number	Definition 1 $h_{avg} = b_1$ (ft)	γ	Definition 2 $h_{avg} = h_{mean}$ (ft)	γ	Definition 3 $h_{avg} = h_{weighted}$ (ft)	γ	Definition 4 $h_{avg} = h(F_{max})$ (ft)	γ
7	0.00	1.00	0.00	1.00	0.00	1.00	0.00	1.00
8	1.00	0.95	0.64	0.98	0.65	0.98	0.74	0.97
9	2.00	0.84	1.27	0.93	1.30	0.92	1.50	0.90
10	2.50	0.76	1.57	0.89	1.61	0.89	1.88	0.85

Table 3b – Moment Arms and Effective Mass Multipliers (Subcompact)

Test Number	Definition 1 $h_{avg} = b_1$ (ft)	γ	Definition 2 $h_{avg} = h_{mean}$ (ft)	γ	Definition 3 $h_{avg} = h_{weighted}$ (ft)	γ	Definition 4 $h_{avg} = h(F_{max})$ (ft)	γ
11	0.00	1.00	0.00	1.00	0.00	1.00	0.00	1.00
12	1.00	0.96	0.65	0.98	0.66	0.98	0.74	0.98
13	2.00	0.86	1.28	0.94	1.32	0.94	1.50	0.92
14	3.00	0.74	1.90	0.88	1.95	0.87	2.27	0.83

Table 3c – Moment Arms and Effective Mass Multipliers (Compact)

Test Number	Definition 1 $h_{avg} = b_1$ (ft)	γ	Definition 2 $h_{avg} = h_{mean}$ (ft)	γ	Definition 3 $h_{avg} = h_{weighted}$ (ft)	γ	Definition 4 $h_{avg} = h(F_{max})$ (ft)	γ
15	0.00	1.00	0.00	1.00	0.00	1.00	0.00	1.00
16	1.00	0.97	0.65	0.99	0.67	0.99	0.75	0.98
17	2.00	0.88	1.33	0.95	1.33	0.94	1.52	0.93
18	3.00	0.77	1.92	0.89	1.97	0.88	2.30	0.85
19	4.00	0.65	2.52	0.82	2.59	0.81	3.08	0.76
20	5.00	0.54	3.07	0.76	3.18	0.75	3.85	0.67

Table 3d – Moment Arms and Effective Mass Multipliers (Intermediate)

Test Number	Definition 1 $h_{avg} = b_1$ (ft)	γ	Definition 2 $h_{avg} = h_{mean}$ (ft)	γ	Definition 3 $h_{avg} = h_{weighted}$ (ft)	γ	Definition 4 $h_{avg} = h(F_{max})$ (ft)	γ
21	0.00	1.00	0.00	1.00	0.00	1.00	0.00	1.00
22	1.00	0.97	0.58	0.99	0.59	0.99	0.65	0.99
23	2.00	0.89	1.15	0.96	1.17	0.96	1.30	0.95
24	3.00	0.78	1.70	0.92	1.74	0.92	1.95	0.90

Table 3e – Moment Arms and Effective Mass Multipliers (Full Size)

For the barrier impact case, M_2 approaches infinity and E_2 approaches zero and the CRASH 3 damage algorithm equations for ΔV, Equations (3) and (4), reduce to the following equation:

$$\Delta V_1 = \sqrt{\frac{2\gamma_1 E_1}{M_1}} \qquad (25)$$

The change in velocity (ΔV) for each simulation was calculated for each of the moment arm definitions. These calculated velocity changes were then compared to the actual ΔVs in Table 2. Table 4 below summarizes the ΔV results obtained from these calculations along with the percent difference between the calculated ΔV and the actual ΔV.

Test Number	Definition 1 ΔV (ft/s)	% Difference	Definition 2 ΔV (ft/s)	% Difference	Definition 3 ΔV (ft/s)	% Difference	Definition 4 ΔV (ft/s)	% Difference
1	10.00	0.27	10.00	0.27	10.00	0.27	10.00	0.27
2	8.05	-12.45	9.25	0.51	9.25	0.51	9.24	0.43
3	60.00	0.27	60.00	0.27	60.00	0.27	60.00	0.27
4	57.13	-0.93	58.10	0.76	58.07	0.70	57.87	0.36
5	50.01	-3.95	53.17	2.12	53.04	1.88	52.25	0.37
6	45.76	-6.02	50.07	2.83	49.89	2.46	48.71	0.02

Table 4a – ΔV Results for Different Average Moment Arm Definitions (Mini)

Test Number	Definition 1 ΔV (ft/s)	% Difference	Definition 2 ΔV (ft/s)	% Difference	Definition 3 ΔV (ft/s)	% Difference	Definition 4 ΔV (ft/s)	% Difference
7	60.00	1.05	60.00	1.05	60.00	1.05	60.00	1.05
8	57.59	-0.80	58.40	0.60	58.37	0.56	58.21	0.27
9	51.42	-3.46	54.16	1.68	54.05	1.48	53.39	0.22
10	47.63	-5.08	51.43	2.50	51.27	2.18	50.26	0.16

Table 4b – ΔV Results for Different Average Moment Arm Definitions (Subcompact)

Test Number	Definition 1 ΔV (ft/s)	% Difference	Definition 2 ΔV (ft/s)	% Difference	Definition 3 ΔV (ft/s)	% Difference	Definition 4 ΔV (ft/s)	% Difference
11	60.00	0.57	60.00	0.57	60.00	0.57	60.00	0.57
12	58.04	-0.61	58.69	0.50	58.67	0.46	58.54	0.24
13	52.89	-2.70	55.15	1.45	55.07	1.30	54.55	0.35
14	46.13	-5.86	50.25	2.54	50.08	2.19	48.97	-0.08

Table 4c – ΔV Results for Different Average Moment Arm Definitions (Compact)

Test Number	Definition 1 ΔV (ft/s)	% Difference	Definition 2 ΔV (ft/s)	% Difference	Definition 3 ΔV (ft/s)	% Difference	Definition 4 ΔV (ft/s)	% Difference
15	60.00	0.70	60.00	0.70	60.00	0.70	60.00	0.70
16	58.31	-0.42	58.87	0.52	58.85	0.49	58.73	0.29
17	53.79	-2.30	55.75	1.26	55.68	1.12	55.21	0.27
18	47.68	-4.99	51.34	2.31	51.18	1.99	50.16	-0.05
19	41.19	-8.19	46.40	3.41	46.15	2.85	44.49	-0.86
20	35.10	-11.80	41.51	4.31	41.17	3.44	38.91	-2.23

Table 4d – ΔV Results for Different Average Moment Arm Definitions (Intermediate)

Test Number	Definition 1 ΔV (ft/s)	% Difference	Definition 2 ΔV (ft/s)	% Difference	Definition 3 ΔV (ft/s)	% Difference	Definition 4 ΔV (ft/s)	% Difference
21	60.00	1.22	60.00	1.22	60.00	1.22	60.00	1.22
22	58.54	-0.53	59.13	0.47	59.12	0.45	59.06	0.34
23	54.59	-2.80	56.70	0.96	56.66	0.89	56.39	0.42
24	49.10	-6.02	53.15	1.74	53.06	1.57	52.48	0.45

Table 4e – ΔV Results for Different Average Moment Arm Definitions (Full Size)

DISCUSSION OF SIMULATION RESULTS

The results reported in Tables 4a through 4e reveal that the greatest accuracy in calculated ΔV is associated with Definition #4 of the collision force moment arm, the moment arm at maximum spring compression. We also observe that Definitions #2, #3, and #4 of the resultant collision force moment arm produce a reasonable level of accuracy. In practice, reconstructionists will inspect and document residual crush, not dynamic maximum crush, and so the collision force moment arm at maximum penetration will not necessarily be accessible to the investigator through observation of the observable damage. Thus, it is significant that any of the last three moment arm definitions produce reasonable accuracy since definitions 2 and 3 more closely approximate the moment arm that could be estimated by inspection of residual damage.

The reader should note that this study tested the *potential* accuracy of the CRASH3 equations in relationship to the effective mass concept. This study has shown that the effective mass concept is a good theoretical construct for modeling the effects of collision force offset. However, this study has not dealt with whether these levels of error can actually be achieved *in practice*. Application of the CRASH3 equations in practice, through the physical inspection and interpretation of impact damage, presents at least two difficulties that could cause inaccurate results, despite the good theoretical foundation for the effective mass concept. First, the reconstructionist must locate the "point" of collision force application. In the simulations of this study, the collision force was applied at a well-defined, easily identified point. During an actual crash, the collision force is distributed over a surface and the investigator will have to decide what point should be used to best represent the location of application of the resultant collision force. Ishikawa has given guidance in relationship to locating the point of collision force application and the reader is referred to his publications for a helpful discussion [3,4]. The second difficulty related to damage interpretation is to determine the direction of the resultant collision force. The literature of accident reconstruction could benefit from a more systematic treatment of damage interpretation in relationship to determining the direction of the resultant collision force.

Finally, it should be noted that there is some numerical error associated with the calculation of the actual ΔVs in Tables 2a through 2e above. This can be seen by examining Table 4a, for instance. For test #1, each of the four moment arm definitions yield a ΔV of 10ft/s. A ΔV of 10ft/s corresponds to the *exact* analytical solution for this case, and yet, Table 4a shows an overprediction of ΔV of 0.27 percent. This is because the "actual" value of ΔV from the numerical simulation was 9.97ft/s (Table 2a), a value that is different than the exact solution. The implication of this is that at least part of the error in calculated ΔV, reported in Tables 4a through 4e, is due to the values of the actual ΔVs themselves. In most cases, the result is that the percent error listed in Tables 4a through 4e are worse than they would be if the numerical simulation was exact.

GENERALIZED CLOSING SPEED FORMULA

Having established that the effective mass concept is theoretically reasonable, the effective mass concept was used to derive a damage energy/closing speed relationship applicable to non-central collisions. This derivation incorporates the same assumptions as the CRASH 3 derivation, including the quasi-one-dimensional nature of the derivation. The implication of the quasi-one-dimensional assumption for the derived damage energy/closing speed relationship is that the closing speed calculated from the resulting formula is the closing speed along the direction of the principle force.

Additional assumptions invoked in the derivation are as follows:

1. Restitution is negligible (e = 0).
2. Initial vehicle yaw velocities are negligible ($\dot{\psi}_{1i} = \dot{\psi}_{2i} = 0$).
3. A common velocity is achieved at the point of collision force transfer.

We start by invoking the principle of conservation of energy, written in a manner valid along the collision force line of action.

$$\frac{1}{2}M_1\dot{X}_{10}^2 + \frac{1}{2}M_2\dot{X}_{20}^2 =$$
$$\frac{1}{2}M_1\dot{X}_{1f}^2 + \frac{1}{2}M_2\dot{X}_{2f}^2 + \frac{1}{2}I_1\dot{\psi}_{1f}^2 + \frac{1}{2}I_2\dot{\psi}_{2f}^2 + E \quad (26)$$

In Equation (26), E is the combined damage energy for both vehicles, $E_1 + E_2$, and $\dot{X}_{10}$ and $\dot{X}_{20}$ are the components of the initial vehicle velocities *along the direction of the principle force*. Also, $\dot{X}_{1f}$ and $\dot{X}_{2f}$ are the vehicle velocities along the direction of the principle force at the time the common velocity is reached at point P, and $\dot{\psi}_{1f}$ and $\dot{\psi}_{2f}$ are the angular velocities, also at the time of common velocity at point P.

Integrating Equation (6) for both vehicles and invoking the assumption that the initial angular velocities are zero, we can show that, at the instant the common velocity is achieved at point P,

$$\dot{X}_{1f} = \dot{X}_P - h_1\dot{\psi}_{1f} \quad (27)$$

and

$$\dot{X}_{2f} = \dot{X}_P - h_2\dot{\psi}_{2f}. \quad (28)$$

From the Newton-Euler equations of motion for the system in Figure 2, combined with Equation (6), it can be shown that

$$\ddot{\psi}_1 = \frac{h_1}{k_1^2}\ddot{X}_1. \quad (29)$$

A similar relationship can be written for Vehicle 2. Integration of Equation (29) over the time period from initial contact until the time the common velocity is reached, assuming the initial angular velocity of the vehicle is zero, yields

$$\dot{\psi}_{1f} = \frac{h_1}{k_1^2}\left(\dot{X}_{1f} - \dot{X}_{10}\right). \quad (30)$$

This equation is equivalent to one derived in Reference 11. Again, a similar equation can be written for Vehicle 2. Substitution of Equations (27), (28), and (30), along

with Equation (30)'s counterpart for Vehicle 2, into Equation (26) leads to Equation (31).

$$\dot{X}_P^2 = \frac{\gamma_1 M_1 \dot{X}_{10}^2 + \gamma_2 M_2 \dot{X}_{20}^2 - 2E}{\gamma_1 M_1 + \gamma_2 M_2} \quad (31)$$

Now, invoke the principle of conservation of linear momentum.

$$M_1\dot{X}_{10} + M_2\dot{X}_{20} = M_1\dot{X}_{1f} + M_2\dot{X}_{2f} \quad (32)$$

Substitution of Equations (27) and (28) into Equation (32) yields

$$M_1\dot{X}_{10} + M_2\dot{X}_{20} =$$
$$M_1\left(\dot{X}_P - h_1\dot{\psi}_{1f}\right) + M_2\left(\dot{X}_P - h_2\dot{\psi}_{2f}\right). \quad (33)$$

Simplifying Equation (33) algebraically, and again invoking Equation (30) and its counterpart, leads to Equation (34).

$$\dot{X}_P = \frac{\gamma_1 M_1 \dot{X}_{10} + \gamma_2 M_2 \dot{X}_{20}}{\gamma_1 M_1 + \gamma_2 M_2} \quad (34)$$

Now, square Equation (34) and equate it with Equation (31) to eliminate $\dot{X}_P$.

$$\frac{\gamma_1 M_1 \dot{X}_{10}^2 + \gamma_2 M_2 \dot{X}_{20}^2 - 2E}{\gamma_1 M_1 + \gamma_2 M_2} =$$
$$\left[\frac{\gamma_1 M_1 \dot{X}_{10} + \gamma_2 M_2 \dot{X}_{20}}{\gamma_1 M_1 + \gamma_2 M_2}\right]^2 \quad (35)$$

Simplifying Equation (35) algebraically leads to Equation (36), which relates the initial closing speed, along the line of action of the collision force, to the damage energy.

$$\dot{X}_{10} - \dot{X}_{20} = \sqrt{\frac{\gamma_1 M_1 + \gamma_2 M_2}{\gamma_1 M_1 \gamma_2 M_2}2E} \quad (36)$$

As an intermediate step in the derivation of Equations (1) and (2), McHenry arrived at the following equation relating the closing speed to the damage energy for the case of central collisions:

$$\dot{X}_{10} - \dot{X}_{20} = \sqrt{\frac{M_1 + M_2}{M_1 M_2}2E} \quad (37)$$

It is clear from comparing Equations (36) and (37) that the only difference between the equation for the central impact case and the equation for the general case of non-central collisions is that the masses in Equation (37)

have been replaced by effective masses in Equation (36). As with McHenry's extension of the CRASH 3 damage analysis equations, the simple, closed-form nature of the central impact damage energy/closing speed Equation has been maintained.

Equation (36) can also be written in terms of the vehicle weights, a form more convenient for application of the Equation, as follows:

$$V_{\text{closingPDOF}} = \sqrt{\frac{\gamma_1 W_1 + \gamma_2 W_2}{\gamma_1 W_1 \gamma_2 W_2} 2gE} \qquad (38)$$

In Equation (38), we have replaced $\dot{X}_{10} - \dot{X}_{20}$ with the notation, $V_{\text{closingPDOF}}$. From this point forward, this new notation will be used to indicate the closing speed projected along the line of action of the collision force, $V_{\text{closingPDOF}}$. This change in notation is necessary, as the following sections aim at transforming the calculated closing speed along the direction of the collision force to a direction more useful for calculating actual vehicle impact speeds.

CLOSING SPEED DIRECTION

The magnitude of the initial closing speed (relative velocity) between two vehicles depends on the line to which that closing speed is referenced. Equation (27) yields the closing speed at impact *projected onto the line of action of the resultant collision force*. Typically, analysis of a motor vehicle accident will require the closing speed along a different reference line, such as the closing speed along the initial velocity direction of one of the vehicles. The speed obtained from Equation (38) will need to be transformed to reflect the closing speed along that different reference line. It should be noted that, in general, impacting vehicles will not have initial velocity vectors along the same line, and so the closing speed will be different depending on which initial velocity direction is used as a reference.

Figure 5 depicts the general geometry of the transformation of the closing speed along the principle direction of force into the closing speed along the initial velocity direction of the first vehicle. Initial velocity vectors are depicted for both vehicles, along with the line of action of the principle force and the angles defining the orientation of the initial velocity directions of the vehicles relative to the principle force line.

Based on geometry and trigonometric identities, it can be shown that, in general,

$$V_{\text{closing,V1}} = V_1 - V_2 \cos(\theta_2 - \theta_1)$$
$$= \frac{V_{\text{closingPDOF}}}{\cos\theta_1} - V_2 \tan\theta_1 \sin(\theta_2 - \theta_1). \qquad (39)$$
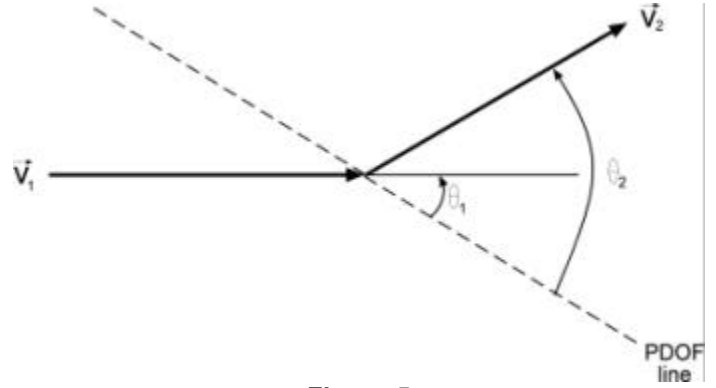
Figure 5
Closing Speed Transformation Geometry

In Equation (39), $V_{\text{closing,V1}}$ is the closing speed projected along the direction of Vehicle 1's initial velocity, V_1 and V_2 are the magnitudes of the vehicles' initial velocities, θ_1 is the angle between the principle direction of force and the initial velocity direction of Vehicle 1, and θ_2 is the angle between the principle direction of force and the initial velocity direction of Vehicle 2. The angles θ_1 and θ_2 are measured counter-clockwise off of the line of action of the principle force.

Equation (39) can be restated as follows:

$$V_1 = \frac{V_{\text{closingPDOF}}}{\cos\theta_1} + V_2[\cos(\theta_2 - \theta_1) - \tan\theta_1 \sin(\theta_2 - \theta_1)] \quad (40)$$

Equation (40) shows that, for the general case, the transformation of the closing speed from the collision force line of action to a reference line coinciding with the initial velocity direction of one of the vehicles, or calculation of the reference vehicle velocity, requires knowledge of the magnitude of the initial velocity of the other vehicle. In practice, this requirement can be met by combining Equations (38) and (40) with an energy balance equation or with a physical constraint on a vehicle's speed. The former, combining Equations (38) and (40) with an energy balance equation, is demonstrated in the next section. As an example of the latter, we can note that the speed of a left-turning vehicle can sometimes be bracketed by consideration of the turn geometry and lateral acceleration capabilities of the vehicle. Also, in some cases, a vehicle's speed will be known from data downloaded from an Event Data Recorder.

When $\theta_2 - \theta_1$ is equal to 0 or 180 degrees, and the closing speed is being calculated, the requirement to know one of the vehicles' absolute speed is relaxed and the transformation is accomplished with Equation (41).

$$V_{\text{closing,V1}} = \frac{V_{\text{closingPDOF}}}{\cos\theta_1} \qquad (41)$$

CONSERVATION OF ENERGY

For a two-vehicle impact, where the vehicles have negligible initial rotational kinetic energy, the principle of conservation of energy can be formulated in the following energy balance Equation:[3]

$$\frac{1}{2} M_1 V_1^2 + \frac{1}{2} M_2 V_2^2 =$$
$$\frac{1}{2} M_1 V_{1f}^2 + \frac{1}{2} M_2 V_{2f}^2 + \frac{1}{2} I_1 \dot\psi_{1f}^2 + \frac{1}{2} I_2 \dot\psi_{2f}^2 + E \qquad (42)$$

In Equation (42), V_{1f} and V_{2f} are the center of gravity velocities when the common velocity is achieved. If the terms on the right side of Equation (42) can be calculated, then Equations (38), (40), and (42) constitute a system of three Equations with three unknowns and the initial vehicle speeds can be calculated. The literature contains extensive discussion of how to quantify the damage energy and post-impact kinetic energy terms and that discussion will not be expanded here. Our discussion here will focus on calculation of the post-impact rotational kinetic energy terms, by relating that rotational kinetic energy to the vehicle inertial properties, the moment arm of the collision force and the damage energy.

Equation (30) can be rewritten as

$$\dot\psi_{1f} = \frac{h_1}{k_1^2} \Delta V_1 \qquad (43)$$

Combining Equation (43) with Equation (3) yields Equation (44).

$$\dot\psi_{1f} = \frac{h_1}{k_1^2} \sqrt{\frac{2\gamma_1 E}{M_1 \left(1 + \frac{\gamma_1 M_1}{\gamma_2 M_2}\right)}} \qquad (44)$$

Equation (44) and its counterpart for Vehicle 2 can be substituted into the rotational kinetic energy terms of Equation (42). Following this substitution, algebraic manipulation yields Equation (45).

$$\frac{1}{2} I_1 \dot\psi_{1f}^2 = \frac{h_1^2}{k_1^2 + h_1^2} \left(\frac{\gamma_1 M_1}{\gamma_1 M_1 + \gamma_2 M_2}\right) E \qquad (45)$$

---

[3] Whereas Equation (26) is only valid when the X-direction coincides with the line of action of the collision force, Equation (42) is independent of the orientation of the inertial reference frame.

A similar relationship can be written for Vehicle 2. Finally, Equation (45) and its counterpart for Vehicle 2 can be substituted into Equation (42) to yield Equation (46).

$$\frac{1}{2} M_1 V_1^2 + \frac{1}{2} M_2 V_2^2 = \frac{1}{2} M_1 V_{1f}^2 + \frac{1}{2} M_2 V_{2f}^2 + \beta E \qquad (46)$$

β is given by Equation (47).

$$\beta = \left[1 + \frac{h_1^2}{k_1^2 + h_1^2}\left(\frac{\gamma_1 M_1}{\gamma_1 M_1 + \gamma_2 M_2}\right) + \frac{h_2^2}{k_2^2 + h_2^2}\left(\frac{\gamma_2 M_2}{\gamma_1 M_1 + \gamma_2 M_2}\right)\right] \qquad (47)$$

Now, when supplemented with techniques for calculating the damage energy and the post-impact kinetic energy, Equations (38), (40), and (46) form a system of three equations with three unknowns and the initial vehicle speeds can be calculated.

CONCLUSIONS

This study has confirmed that, as long as a reasonable representative collision force moment arm can be obtained, the effective mass concept accurately captures the effects of collision force offset. The greatest accuracy is achieved by selecting the representative moment arm of the collision force as close to maximum deformation as possible. A damage energy/closing speed relationship was derived for the general case of non-central collisions, where the line of action of the collision forces does not pass through the vehicle centers of gravity. Second, this generalized damage energy/closing speed relationship was integrated with an energy balance equation, via a derived relationship between damage energy and post-impact rotational kinetic energy, to provide a complete set of equations for vehicle speed analysis.

REFERENCES

1. Baruh, Haim, Analytical Dynamics, WCB/McGraw-Hill, 1999.

2. Beer and Johnston, Vector Mechanics for Engineers, Fifth Edition, McGraw-Hill Book Company, New York, 1988.

3. Ishikawa, Hirotoshi, "Impact Model for Accident Reconstruction – Normal and Tangential Restitution Coefficients," 930654, Society of Automotive Engineers, Warrendale, PA, 1993.

4. Ishikawa, Hirotoshi, "Impact Center and Restitution Coefficients for Accident Reconstruction," 940564, Society of Automotive Engineers, Warrendale, PA, 1994.

5. McHenry, "A Comparison of Results Obtained with Different Analytical Techniques for Reconstruction of

Highway Accidents," 750893, Society of Automotive Engineers, Warrendale, PA, 1975.

6. McHenry, Raymond R., "Extensions and Refinements of the CRASH Computer Program Part II," DOT HS-801 838, February, 1976.

7. McHenry, Raymond R., Jones, Ian S., "Extensions and Refinements of the CRASH Computer Program Part III, Evaluation of the Accuracy of Reconstruction Techniques for Highway Accidents," DOT HS-801 839, February, 1976.

8. McHenry and Lynch, "Mathematical Reconstruction of Highway Accidents – Further Extensions and Refinements of the CRASH Computer Program," Calspan, 1976.

9. McHenry, Raymond R., "Computer Aids for Accident Investigation," 760776, Society of Automotive Engineers, Warrendale, PA, 1976.

10. Siddall, Donald E., Day, Terry D., "Updating the Vehicle Class Categories," 960897, Society of Automotive Engineers, Warrendale, PA, 1996.

11. Varat, Michael S., Husher, Stein E., "Vehicle Crash Severity Assessment in Lateral Pole Impacts," 1999-01-0100, Society of Automotive Engineers, Warrendale, PA, 1999.

CONTACT INFORMATION

The authors welcome comments and questions and can be reached at the address, phone number, or email address below.

Knott Laboratory, Inc.
7185 South Tucson Way
Englewood, Colorado 80112
(303) 925-1900
(303) 925-1901 Fax
nrose@knottlab.com